

# Tree ring based precipitation reconstruction in the south slope of the middle Qilian Mountains, northeastern Tibetan Plateau, over the last millennium

Junyan Sun<sup>1</sup> and Yu Liu<sup>1,2</sup>

Received 7 December 2011; revised 10 February 2012; accepted 4 March 2012; published 24 April 2012.

[1] A tree ring (*Sabina przewalskii* Kom.) based millennial precipitation reconstruction on the south slope of the middle Qilian Mountains in the northeastern margin of Tibetan Plateau, China, was completed, which explains 48.5% of the variance in the instrumental precipitation from 1958 to 2004. The long-term precipitation variation patterns were confirmed on the basis of the duration, magnitude, and intensity of the multidecadal dry (wet) events. There are several stronger multidecadal dry periods, 1092–1172, 1441–1517, and 1564–1730, whereas there is only one outstanding severe wet event of 1352–1440. The variations of the precipitation reconstruction are accordant with the glacier accumulation and dust contents of Dunde ice core and also with the variations of the precipitation, runoff, Palmer Drought Severity Index, and tree ring width series in the northeastern Tibetan Plateau. The spatial extent of the great drought in the latter half of the 15th century also concentrated on the northeastern Tibetan Plateau. The moisture variations in the northeastern Tibetan Plateau are synchronous over a large spatial and temporal range in multidecadal scale for the last millennium, especially during dry periods. Wavelet analyses and comparisons with the minimal solar activity show that the precipitation variations for the last millennium may have some association with the solar activity on multidecadal to centennial scales.

**Citation:** Sun, J., and Y. Liu (2012), Tree ring based precipitation reconstruction in the south slope of the middle Qilian Mountains, northeastern Tibetan Plateau, over the last millennium, *J. Geophys. Res.*, 117, D08108, doi:10.1029/2011JD017290.

## 1. Introduction

[2] Worldwide instrumental climate data are only available for approximately one century. Therefore, it is necessary to use proxy climate indicators in combination with the available instrumental records to gain insights into the large-scale climate variability that occurred during the last millennium [Mann and Jones, 2003]. Owing to its high time resolution, precise dating and sensitivity to climate signals, tree ring has been one of the most important proxy indicators for studying past climate [e.g., Jones *et al.*, 1998; Crowley, 2000; Briffa *et al.*, 2001; Esper *et al.*, 2002; Mann and Jones, 2003; Shao *et al.*, 2005; D'Arrigo *et al.*, 2006; Liu *et al.*, 2006; Gou *et al.*, 2007; Qin *et al.*, 2010].

[3] The Tibetan Plateau is the highest and largest plateau on Earth and is one of the regions in the world that is sensitive to global change [Liu and Chen, 2000]. There have

been several millennial climate reconstructions. These reconstruction series played an important role in the previous and future climate researches in this region [Zhang *et al.*, 2003; Liu *et al.*, 2005; Shao *et al.*, 2005; Liu *et al.*, 2006, 2009; Gou *et al.*, 2007; Qin *et al.*, 2010].

[4] The Qilian Mountains are located in the northeastern margin of the Tibetan Plateau. More than 70 rivers originate from the Qilian Mountains, where is a significant water resource conservation area for the arid and semiarid regions of China and also the lifeline of the Heixi Corridor oasis [Jia *et al.*, 2008]. So it is critical important to acquire the moisture variations (especially the drought history) in the Qilian Mountains. The long-living and climate-sensitive trees in the Qilian Mountains allow for the reconstruction of the history climate variations in this region. Several climatic and hydrological analyses have been published based on tree ring data from the Qilian Mountains [Gou *et al.*, 2005; Liu *et al.*, 2005; Tian *et al.*, 2007; Liu *et al.*, 2010; Qin *et al.*, 2010]. However, few reconstructed precipitation series exceeded millennial scale, and we still have no idea of the detailed information of the history precipitation variation (dry and wet period) patterns in the Qilian Mountains and their regional representativeness. The aim of present study is to reconstruct the precipitation variations for the last millennium using samples from the south slope of the middle Qilian Mountains (SMQL); characterize the

<sup>1</sup>State Key Laboratory of Loess and Quaternary Geology, Institute of Earth Environment, Chinese Academy of Sciences, Xi'an, China.

<sup>2</sup>Department of Environmental Science and Technology, School of Human Settlements and Civil Engineering, Xi'an Jiaotong University, Xi'an, China.

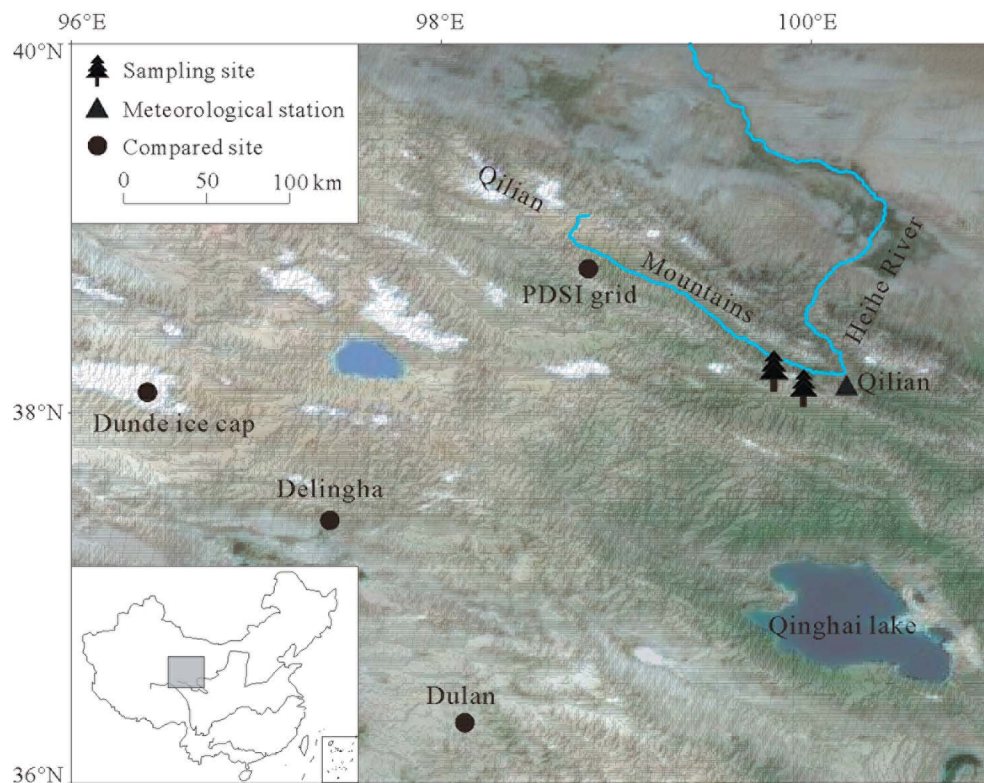


**Figure 1.** Locations of the sampling sites (trees), the meteorological station (triangle), and the compared sites (dots).

precipitation variation patterns and their regional representativeness.

## 2. Materials and Methods

### 2.1. Study Area and Tree Ring Chronology

[5] The Qilian Mountains are located between  $93^{\circ}31'$  to  $103^{\circ}00'E$  and  $36^{\circ}30'$  to  $39^{\circ}30'N$  and stretch for 850 km from northwest to southeast with a width of 200 to 300 km (Figure 1). The altitudes of the Qilian Mountains range between 3000 to 5000 m a.s.l. and are higher in the northwest than in the southeast. The Qilian Mountains are located in the northeastern margin of Tibetan Plateau and the climate is influenced by both the Asian monsoons and the westerlies [Ji *et al.*, 2005; Zhang *et al.*, 2007; Qin *et al.*, 2010]. According to the climate data of Qilian meteorological station, the mean annual temperature is  $+0.9^{\circ}C$ , with a January average of  $-13^{\circ}C$  (coldest) and a July average of  $+13^{\circ}C$  (warmest). The mean annual precipitation is 403 mm, and the majority of the precipitation in this region falls between June and August (Figure 2). The dominant tree species in the study area were *Sabina przewalskii* Kom. and *Picea crassifolia* Kom.

[6] Standard dendrochronological techniques were employed for the present analysis [Fritts, 1976; Holmes, 1983; Cook and Kairiukstis, 1990; Stokes and Smiley, 1996]. Two sampling sites were selected in the Qilian Mountains (Figure 1) where little apparent anthropogenic influence exists. The samples were taken from isolated living trees in a homogeneous microenvironment and were characterized by few nonclimatic disturbances. Almost all of the samples were collected from trees

on steep slopes or cliffs where tree growth is more sensitive to moisture stress [Douglass, 1919; Fritts, 1976]. The first sampling site is located at  $99^{\circ}47'E$ ,  $38^{\circ}14'N$  (3300 m a.s.l.). At this site, 44 increment cores were sampled from 22 trees. The second site is located at  $99^{\circ}57'E$ ,  $38^{\circ}09'N$  (3300 m a.s.l.) and 50 increment cores were sampled from 25 trees in this site. All of the increment cores were taken from the same tree species (*Sabina przewalskii* Kom.).

[7] After dried, mounted and progressively sanded, all of the samples were cross-dated using skeleton plots [Stokes and Smiley, 1996], and each individual ring was accurately assigned a calendar year. The cross-dated tree rings were measured using a Lintab tree ring width measuring system with a 0.001 mm precision. The quality of the cross-dating was controlled using COFECHA program [Holmes, 1983]. The series intercorrelation of all the raw ring width measurements in two sampling sites was 0.60 ( $p < 0.001$ ). In addition, two sites have close proximity and homogeneous environment. Then all of the raw measurement data were combined into one group to identify the expected regional climate signals for the subsequent study. In total, 94 cores from 47 trees were used for further analyses.

[8] The tree ring width chronology was developed using the ARSTAN program [Cook and Kairiukstis, 1990] by fitting a conservative method, employing negative exponential curves or straight lines. The standard chronology developed by ARSTAN program was using in this research. As is generally the case in dendroclimatic studies, the quality of the chronology weakens during the early period owing to a decreasing sample depth, the subsample signal strength was used to assess the adequacy of the replications in the early

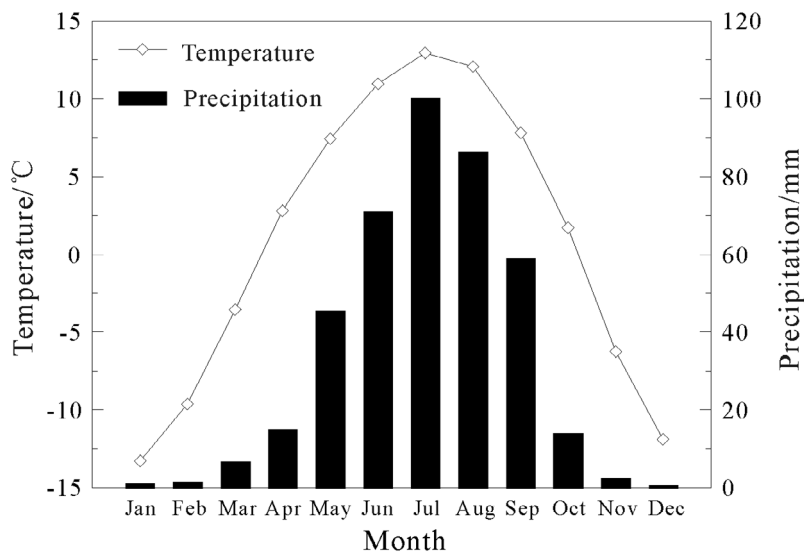


**Figure 2.** Average monthly precipitation and temperature at the Qilian meteorological station.

years of the chronology [Wigley *et al.*, 1984]. In the present paper, we used the subsample signal strength with a threshold value of 0.80, which corresponds to a minimum sample depth of six trees from 1063 AD. The express population signal, which indicates the degree to which the particular sample chronology portrays a hypothetically perfect chronology [Wigley *et al.*, 1984], exceeded 0.92. This is well above the 0.85 threshold value that is considered acceptable by the field [Wigley *et al.*, 1984; Cook and Kairiukstis, 1990; Pederson *et al.*, 2001]. The final reliable chronology extends from 1063 to 2009 AD.

## 2.2. Climatic Data

[9] The nearest meteorological station to sampling sites is the Qilian station (1957–2004). The Qilian meteorological station is located at 100°15'E, 38°11'N (2790 m a.s.l.). The local monthly mean temperature and precipitation records from the Qilian meteorological station was used in our analysis. Figure 2 shows the monthly mean temperature and precipitation of the Qilian meteorological station.

## 2.3. Statistical Methods

[10] The relationships between the climatic factors and tree growth were investigated using software DENDROCLIM 2002 [Biondi and Waikul, 2004], which used bootstrap confidence intervals to estimate the significance of the correlation function coefficients [Mudelsee, 2003; Biondi and Waikul, 2004]. Then the simple linear regression model was used for seasonal precipitation reconstruction.

[11] The Bootstrap [Efron, 1979; Young, 1994] and Jackknife statistical methods [Mosteller and Tukey, 1977] were used for verification. The Bootstrap, introduced by Efron, was hailed as the latest important work in the field of time series statistics [Efron, 1979]. The original data are resampled many times to simulate sampling variability and to provide an approximation for the unknown population by using the Bootstrap method. The Jackknife relies on leaving out one observation in the calibration period at a time, and then the statistic desired is computed on the remainder [Gordon, 1980]. We also used the sign test ( $S_2$ ), the sign test of the

first difference ( $S_1$ ), the product mean ( $t$ ) and the reduction of error (RE) [Fritts, 1976] to verify the reconstruction.

## 3. Results

### 3.1. Correlation Analyses Between the Tree Ring Chronology and Climate Data

[12] The climate-growth correlation function analyses were performed between the standard tree ring chronology and the monthly precipitation and temperature at Qilian meteorological station from previous April to current August [Fritts, 1976; Shao *et al.*, 2005]. As shown in Figure 3, the tree ring chronology has significant negative correlations at the 95% confidence level with the temperatures in current May and July and has significant positive correlation at the 95% confidence level with the temperature of previous November. Contrast to temperature, the tree ring chronology exhibits significant positive correlations at the 95% confidence level with the precipitation in previous August, current May and June (Figure 3).

[13] The various multimonth average temperature and total precipitation were combined to obtain the seasonal effects, including prior winter temperature, growth season temperature, growth season precipitation and annual precipitation (dendroclimatic year from previous July to current June). The highest correlation coefficient between the tree ring chronology and seasonal precipitation is 0.70 ( $p < 0.05$ ), acquired in a full dendroclimatic year from previous July to current June. Another higher correlation coefficient, between tree growth and the precipitation of current May to June, is 0.45 ( $p < 0.05$ ). For temperature, the highest correlation is between the tree ring chronology and average temperature from May to July with a value of  $-0.43$  ( $p < 0.05$ ). Another significant positive correlation is between tree ring chronology and winter temperature, from previous November to current January, with a value of 0.33 ( $p < 0.05$ ).

[14] The pregrowth and growth season precipitation positively correlated with tree growth, while the growth season temperature negatively correlated with tree growth. This

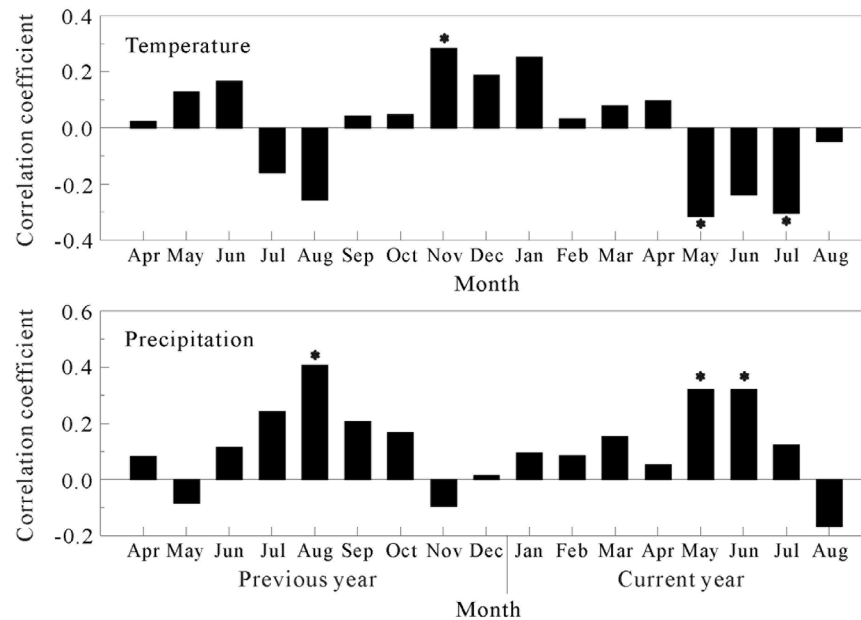


**Figure 3.** Correlation function analyses for the tree ring chronology and the monthly precipitation and temperature at the Qilian meteorological station (1958–2004). Asterisks indicate significance at the 95% confidence level; both the tree ring chronology and climate data are annually resolved series.

demonstrated that tree growth in study site is moisture stressed [Fritts, 1976; Shao *et al.*, 2005]. The precipitation of the full dendroclimatic year from previous July to current June is the most important factor limiting tree growth in study site. This finding is consistent with other juniper sites in the northeastern Tibetan Plateau, Dulan [Sheppard *et al.*, 2004; Liu *et al.*, 2006], and Delingha [Shao *et al.*, 2005]. It should be noted, although the dendroclimatic year precipitation plays the most important role on the tree growth, the winter temperature still has some effects.

### 3.2. Precipitation Reconstruction in SMQL From 1063 to 2009

[15] Based above climate-growth correlation function analyses, the precipitation period from previous July to current June was chosen for reconstruction using linear regression model. The regression model and related statistical parameters are contained in Table 1. The dependent variable  $P$  in Table 1 is the total precipitation from previous July to current June, and the independent variable  $W_t$  is the associated tree ring width chronology of year  $t$ . D/W is the Durbin-Watson value, which is used to detect the presence of an autocorrelation in the residuals of the regression models. When the sample size is  $n = 47$ , no autocorrelation exists with a D/W value between 1.59 and 2.41 [Durbin and Watson, 1951].

[16] During the calibration period of 1958 to 2004, the predictor variable accounts for 48.5% of the variance in the observed precipitation (47.4% after the adjustment for the loss of degrees of freedom). Figure 4 shows the comparison of the observed and reconstructed precipitation in SMQL during the calibration period. The reconstructed values match the observed values particularly well before 1985. While there is an underestimation of wet and dry years after 1985 compared to the relationship prior to 1985. This

may attribute to the trend distortion at the end of the chronology [Melvin and Briffa, 2008].

[17] Because the observed climate data are relatively short, only 47 years, the data were not divided into two subperiods for calibration and verification of the dendroclimatic model [Jacoby *et al.*, 1999; Sheppard *et al.*, 2004]. The Bootstrap [Efron, 1979; Young, 1994] and Jackknife statistical methods [Mosteller and Tukey, 1977] were used to verify the stability of the transfer function and the reliability of precipitation reconstruction. The results obtained using the Bootstrap (400 iterations in the resampling process) [Efron and Tibshirani, 1993] and Jackknife methods reveal that all of the values of the  $r$ ,  $r^2$ ,  $r_{adj}^2$ , standard error ( $\sigma$ ),  $t$ -value,  $F$ -value,  $p$ -value and D/W statistics were similar to the values of the original data set (Table 2).

[18] The sign test ( $S_1$ ,  $S_2$ ), the product mean ( $t$ ) and the reduction of error (RE) [Fritts, 1976] were also used to verify the precipitation reconstructions, and the results are listed in Table 3. Except that the sign test  $S_2$ , significant at

**Table 1.** Regression Model and the Related Statistical Parameters<sup>a</sup>

Parameter	Value
<i>Regression Model of the Precipitation Reconstruction in SMQL</i>	
$P$	$202.206^*W_t + 202.58$
<i>Related Statistical Parameters of the Regression Model</i>	
$n$	47
$r$	0.70
$R^2$	48.5%
$R_{adj}^2$	47.4%
$F$	42.45
$p$	<0.0001
D/W	1.76

<sup>a</sup> $P$  is the total precipitation from previous July to current June.  $W_t$  is the associated tree ring chronology of year  $t$ . D/W is the Durbin-Watson value.

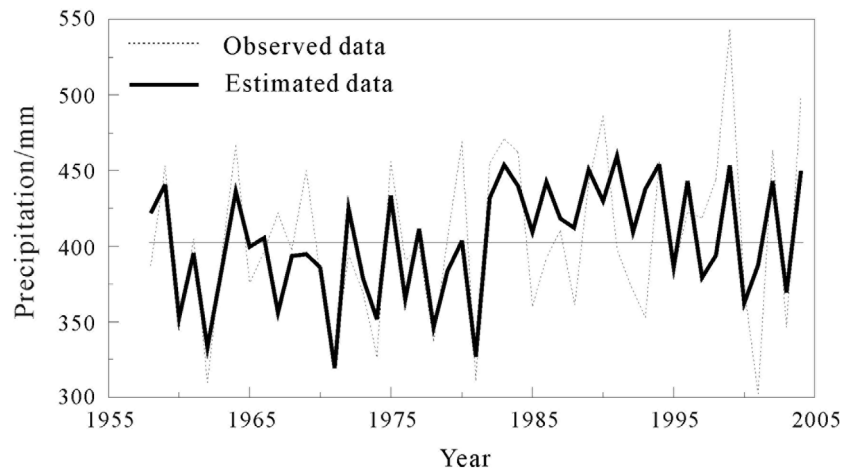


**Figure 4.** Comparison of the observed (dotted line) and reconstructed (solid line) precipitation from previous July to current June in SMQL during the calibration period of 1958 to 2004; the horizontal line is the mean of the observed data.

95% confidence level, all the other statistical items are significant at the 99% level.

[19] These verification tests indicate that the regression model for the study region is stable and reliable and is deemed acceptable to reconstruct the precipitation from previous July to current June in SMQL for AD 1063–2009 on the basis of the millennial tree ring chronology.

## 4. Discussion

### 4.1. Long-Term Precipitation Variations Over the Last Millennium

[20] The thin line in Figure 6a demonstrates the precipitation reconstruction. The smoothed (40 year cubic smoothing spline [Cook and Peters, 1981]) line shows some decadal-scale dry (wet) regimes. To identify and characterize different modes of the long-term precipitation variations for the last millennium, the successive years with the smoothed precipitation below (above) the mean of the reconstruction (401 mm) were defined as the dry (wet) events. Then the dry (wet) regimes were assessed on the basis of their duration, magnitude, and intensity [Biondi *et al.*, 2002; Gray *et al.*, 2004, 2011]. Duration is the total numbers of continuous years of the individual wet or dry regimes. Magnitude is the cumulative departure of the precipitation for any given duration. Intensity is the ratio between magnitude and duration [Biondi *et al.*, 2002]. Finally the event score was

assigned as the sum of the ranking for duration, absolute magnitude and absolute intensity [Biondi *et al.*, 2002; Gray *et al.*, 2004, 2011]. The wet and dry regimes of the precipitation reconstruction in SMQL were scored separately in Table 4, the higher the event score, the stronger the event.

[21] On the basis of event scores, the two most severe droughts experienced in SMQL during the last millennium are 1092–1172 and 1564–1730. Although these two strong droughts have the same highest score, they have different dry pattern. The drought ending in 1730 has the longest duration and highest magnitude, with a bit lower intensity, whereas the drought roughly in 12th century is a prolonged, severe drought with the second ranking duration, magnitude and intensity. The second scored drought is from 1441 to 1517. Similar with the drought in 12th century, this drought also is a prolonged, severe drought. Both of the two lowest scored dry events, 1215–1229 and 1942–1977, have quite low intensity; and the average precipitation of these two regimes are 403 mm and 394 mm, very close to the reconstruction mean. So they are not the strictly dry events. Almost all of the multidecadal dry events in Table 4 are accordant with the precipitation reconstructions (total precipitation from previous July to current June) in Delingha [Shao *et al.*, 2005] and Dulan [Sheppard *et al.*, 2004; Liu *et al.*, 2006], 280 km southwest away from study region (Figures 1 and 6). Such as the most severe drought from 1564 to 1730 corresponds to the driest period (1588–1717)

**Table 2.** Verification Results of the Bootstrap and Jackknife Methods for the SMQL Regression

Statistical Items	Calibration Period	Verification Period	
		Bootstrap: Mean <sup>a</sup>	Jackknife: Mean <sup>a</sup>
$r$	0.70	0.70 (0.55–0.81)	0.70 (0.67–0.73)
$r^2$	0.49	0.48 (0.30–0.66)	0.49 (0.45–0.53)
$r_{adj}^2$	0.47	0.47 (0.29–0.65)	0.47 (0.44–0.52)
Standard error ( $\sigma$ )	39.22	38.44 (32.79–44.6)	39.22 (37.14–39.67)
$t$	6.51	6.53 (4.57–8.66)	6.38 (5.89–7.13)
$F$	42.45	45.32 (19.38–87.13)	41.59 (36.28–50.12)
$p$	0.0001	0.0001 (0.001–0.0001)	0.0001 (0.0001–0.0001)
D/W	1.76	1.72 (1.54–1.94)	1.76 (1.63–1.97)

<sup>a</sup>Values in parentheses are intervals.

**Table 3.** Statistical Characteristics of the Verification of the Precipitation Reconstruction [Fritts, 1976]<sup>a</sup>

Statistical Items	Value
S <sub>1</sub>	39 (31 <sup>b</sup> , 33 <sup>c</sup> )
S <sub>2</sub>	31 (31 <sup>b</sup> , 33 <sup>c</sup> )
<i>t</i>	5.04
RE	0.48
<i>n</i>	47

<sup>a</sup>S<sub>1</sub> is the sign test of the first difference, and S<sub>2</sub> is the sign test.

<sup>b</sup>Significant at the 95% confidence level.

<sup>c</sup>Significant at the 99% confidence level.

in Dulan [Liu *et al.*, 2006] (Figure 1); and the severe drought from 1441 to 1517 corresponds to the driest period (1465–1495) in Delingha [Shao *et al.*, 2005] (Figure 6).

[22] The highest scored wet events during the last millennium occurred from 1352 to 1440, which is a prolonged, strong wet period with the highest scored duration, magnitude and intensity. Although the wet from 1731 to 1813 has the second score and similar duration, its magnitude and intensity are just half of that of the wet from 1352 to 1440. Other wet events have lower duration, magnitude and intensity. So the wet from 1352 to 1440 is an outstanding wet event among all high-precipitation intervals. Owing to the approximate mean precipitation value to the reconstruction mean and the slightest intensity, the lowest scored wet event from 1173 to 1214 is not the wet event in the strict sense. Similar to the dry events, almost all of the multi-decadal wet events in Table 4 are also synchronous with other precipitation reconstruction in Delingha and Dulan [Sheppard *et al.*, 2004; Shao *et al.*, 2005; Liu *et al.*, 2006] (Figure 6).

[23] The multidecadal dry and wet events were also compared to the high- and low-flow periods of the reconstructed runoff in the Heihe River which originates from the Qilian Mountains [Qin *et al.*, 2010] (Table 5). Except for three intervals with approximate mean precipitation value to the reconstruction mean (1215–1229, 1942–1977 and 1173–

**Table 5.** Comparison Between the Dry and Wet Intervals of the Precipitation Reconstruction in SMQL and the Runoff Reconstruction of the Heihe River [Qin *et al.*, 2010]

Precipitation	Runoff
<i>Dry Intervals</i>	
1092–1172	1104–1212
1311–1351	1259–1352
1441–1517	1442–1499
1564–1730	1593–1739
1814–1878	1789–1884
<i>Wet Intervals</i>	
1071–1091	1054–1103
1230–1310	1213–1258
1352–1440	1353–1441
1518–1563	1500–1592
1731–1813	1740–1788
1879–1941, 1978–2004	1885–2008

1214), the long-term variations of the reconstructed precipitation in SMQL are in agreement with the reconstructed runoff of the Heihe River.

[24] The analyses above depict the detailed patterns of the long-term precipitation variations for the last millennium in SMQL. The dry and wet intervals comparisons confirm the reliability of the precipitation reconstruction and reveal the potential consistency of the precipitation variation in the northeastern Tibetan Plateau.

#### 4.2. Comparisons and Regional Representativeness

[25] The precipitation reconstruction in SMQL was compared with the glacier accumulation [Yao *et al.*, 1991] and dust content [Liu *et al.*, 1999] in the Dunde ice cap. The Dunde ice cap (96°24'E, 38°06'N) is also located in the northeastern Tibetan Plateau (Figure 1). The variations of the precipitation reconstruction are accordant with the glacier accumulation of Dunde ice core since 1600 AD (solid line in the top of Figure 5). Comparisons between the precipitation reconstruction and dust content in Dunde ice

**Table 4.** The Long-Term Dry and Wet Periods Against the Mean of Precipitation Reconstruction Since 1063 AD<sup>a</sup>

Score	Periods	Average <i>P</i>	Duration	Rank	Magnitude	Rank	Intensity	Rank
<i>Dry Events</i>								
21	1092–1172	378.4	81	7	–2057.7	7	–25.4	7
21	1564–1730	384.2	167	8	–3262.3	8	–19.5	5
18	1441–1517	380.2	77	6	–1811.4	6	–23.5	6
13	1814–1878	389.4	65	5	–935	5	–14.4	3
12	1311–1351	389.2	41	4	–596.3	4	–14.5	4
11	1063–1070	375.3	8	1	–227.5	2	–28.4	8
8	1942–1977	394.7	36	3	–324.9	3	–9	2
4	1215–1229	403.4	15	2	–5.2	1	–0.3	1
<i>Wet Events</i>								
24	1352–1440	430.1	89	8	2340.7	8	26.3	8
18	1731–1813	417	83	7	1100.1	7	13.3	4
16	1879–1941	417.9	63	5	892	5	14.2	6
15	1230–1310	415.9	81	6	980.6	6	12.1	3
15	1518–1563	420.3	46	4	759.2	4	16.5	7
9	1071–1091	417.7	21	1	291.6	3	13.9	5
6	1978–2004	414	27	2	274.9	2	10.2	2
5	1173–1214	406.2	42	3	101.8	1	2.4	1

<sup>a</sup>Average *P* is average previous July to current June precipitation over dry or wet regimes. Duration is the total numbers of continuous years of the individual wet or dry regimes. Magnitude is the cumulative departure of the precipitation for any given duration (departure from mean of the precipitation reconstruction since 1063 AD). Intensity is the ratio between magnitude and duration. The event score is the sum of the ranking of duration, absolute magnitude, and absolute intensity (higher scores indicate stronger events [Biondi *et al.*, 2002]).

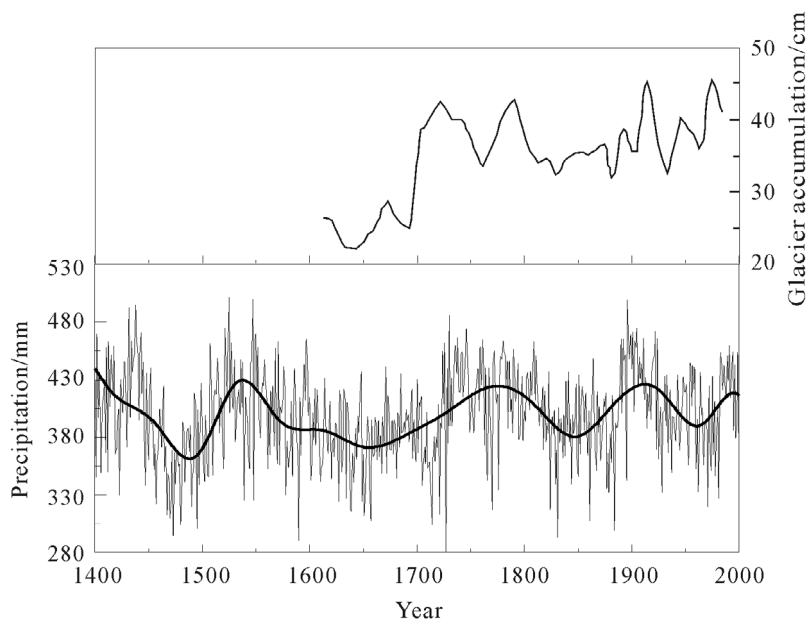


**Figure 5.** Comparison between the precipitation reconstruction in SML and the glacier accumulation in the Dunde ice cap [Yao *et al.*, 1991].

core after 1400 AD demonstrate that lower-precipitation periods roughly correspond to higher dust content periods (1430–1520, 1580–1710, 1770–1880) and higher-precipitation periods correspond to lower dust content periods (1520–1580, 1710–1770, 1880–1980) [Liu *et al.*, 1999]. The relationships between them may result from that dry moisture conditions lead to higher blown dust, and vice versa. The consistencies between the precipitation with the glacier accumulation and dust content confirm the reliability of our reconstruction.

[26] To acquire the regional representativeness, the reconstructed precipitation was compared with other millennial tree ring index series or precipitation reconstruction series in Delingha [Shao *et al.*, 2005] (Figure 6b) and Dulan [Zhang *et al.*, 2003; Liu *et al.*, 2006] (Figures 6c and 6d). These two sites are also located in the northeastern Tibetan Plateau. The details of three compared series are listed in Table 6, and the corresponding study regions are marked in Figure 1. The compared series from Shao *et al.* [2005] in Delingha and Liu *et al.* [2006] in Dulan are both precipitation reconstruction from previous July to current June. The compared series from Zhang *et al.* [2003] in Dulan is the tree ring index which mainly reflects variations in regional precipitation from current May to June. As shown in Figure 6, the reconstructed precipitation could be compared to these series, especially during the dry period. This indicates that the precipitation in the northeastern Tibetan Plateau has similar variations over a large spatial and temporal range.

[27] Cook *et al.* [2010] developed the Monsoon Asia Drought Atlas (MADA) which is composed of the absolutely dated, annually resolved Palmer Drought Severity Index (PDSI) reconstruction ( $2.5^\circ \times 2.5^\circ$  grid) from AD 1300 to 2005. The precipitation reconstruction was also compared with one nearest PDSI series ( $98^\circ 45'E$ ,  $38^\circ 45'N$ , marked in Figure 1) from the MADA [Cook *et al.*, 2010] in Figure 6, and the results indicated that both of them have synchronous variation in decadal scale. The 40 year moving correlation function analyses indicates that the higher

moving correlation coefficients ( $r > 0.40$ , significant at 99% confidence level) mainly distribute in three stages, before 1348, from 1447 to 1510 and after 1630. The lower moving correlation coefficient periods approximately correspond to the two highest intensity wet events.

[28] To further reveal the regional response, we calculated the spatial correlations between the precipitation reconstruction and the entire grid network of MADA [Cook *et al.*, 2010] (Figure 7a). All of the compared series in Figure 7a were smoothed by 40 year cubic smoothing spline. The results show that the highest positive correlation coefficients, in red, mostly distribute in the northeastern Tibetan Plateau, which indicates the climatic consistency in the northeastern Tibetan Plateau. Thompson *et al.* [2006] demonstrated the climatic dichotomy, divided by  $\sim 33^\circ N$ , in the Tibetan Plateau based on four ice cores in the northern and southern Tibetan Plateau. As shown in Figure 7a, the higher correlation coefficients also concentrate on the region north of  $33^\circ N$ , which further confirms the argument of climatic dichotomy in the Tibetan Plateau.

[29] The comparisons between the precipitation reconstruction and PDSI data from MADA demonstrate that the multidecadal-scale moisture variations are synchronous in the northeastern Tibetan Plateau; the drought periods have more synchronism than wet periods.

#### 4.3. The Great Drought During the Latter Half of the 15th Century in the Northeastern Tibetan Plateau

[30] As shown in Figure 6, the great drought from 1440 to 1517 has been depicted by almost all of the five series in the northeastern Tibetan Plateau. The reconstructed annual precipitation indicates that the continuous dry years mainly concentrated on the latter half of the 15th century. This drought event lasted for half a century and has been recorded by several historical documents, such as the disaster history of northwestern China [Yuan, 1994]. The disaster history of northwestern China quantified the history disasters using

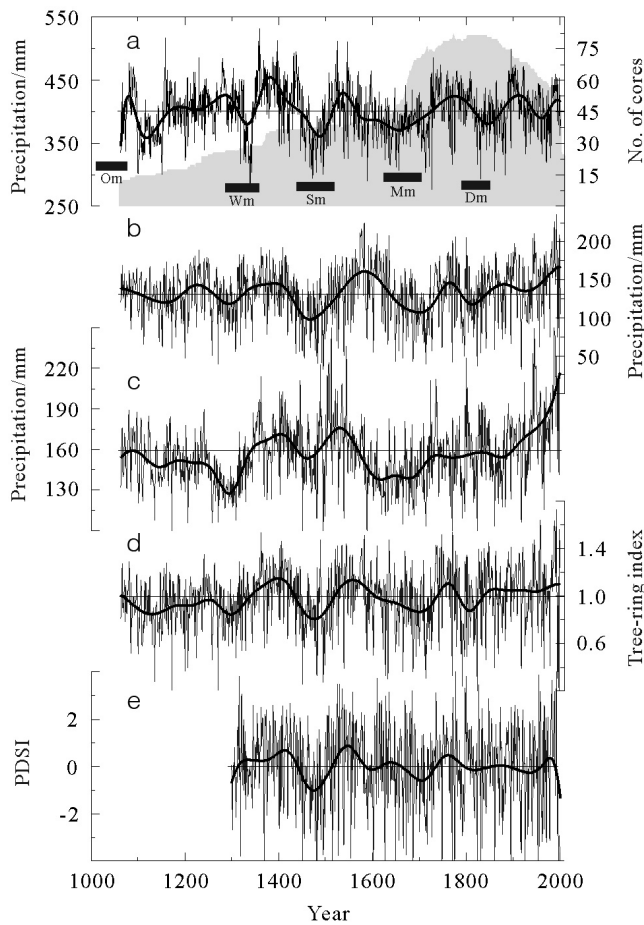


**Figure 6.** (a) The reconstructed precipitation from previous July to current June since 1063 AD in SMQL; the shaded portion is the number of samples, and the black rectangles correspond to the five minima of solar activity. Om, Oort Minimum; Wm, Wolf Minimum; Sm, Spoerer Minimum; Mm, Maunder Minimum; and Dm, Dalton Minimum. (b) The tree ring based precipitation reconstruction from previous July to current June in Delingha [Shao *et al.*, 2005]. (c) The tree ring based precipitation reconstruction from previous July to current June in Dulan [Liu *et al.*, 2006]. (d) The tree ring width series in Dulan [Zhang *et al.*, 2003]. (e) The Palmer Drought Severity Index (PDSI) series from the MADA (98°45'E, 38°45'N) [Cook *et al.*, 2010]. The smoothed lines are the 40 year cubic smoothing spline.

numerous historical documents and the dry situations in northwest China were denoted using grades A to E, indicating light drought to extreme drought. Very few destructive droughts were denoted as F+ [Yuan, 1994]. As recorded, there are 42 dry years during the period 1450 to 1499. Among these 42 dry years, there are 22 years that the dry situations are C or greater than C (including 10 years of grade E and 2 destructive drought years of grade F+). The reconstructed dry years from 1450 to 1499 with lower precipitation than the millennial mean in SMQL are 44 years, among which 37 years have been recorded as dry years in the disaster history of northwestern China. There is a major drought with 28 consecutive dry years from AD 1465 to 1492 in the annual-scale precipitation reconstruction. These indicate that the drought during the latter half of the 15th century is a long-lasting severe drought.

[31] Here, we also used the MADA to identify the regional footprint and severity of the great drought during the latter half of the 15th century. This drought is sharply expressed in northeastern Tibetan Plateau with lower PDSI value in brown in Figure 7b. The comparison with the MADA provides a more complete spatial context of the drought in the latter half of the 15th century and further confirms the synchronous occurrence of drought in the northeastern Tibetan Plateau.

#### 4.4. Periodicity Analysis and the Potential Relationship Between the Precipitation Variation and Solar Activity for the Last Millennium

[32] Wavelet analysis was employed to identify the periodicity of the precipitation in SMQL for the last millennium [Torrence and Compo, 1998]. Figure 8 shows the wavelet analysis results for the precipitation reconstruction since 1063 AD with cone of influence (cross-hatched regions) and significance levels contour of 95%. The dominant periodicities of the precipitation are around 2–3, 39, 60–79, 104–209 years. The interannual cycles of 2–3 years have been found in many tree ring based climate reconstructions [Pederson *et al.*, 2001; Gou *et al.*, 2007; Qin *et al.*, 2010]. The cycle of 39 years is similar to the Bruckner cycle [Raspovov *et al.*, 2004]. The multidecadal cycles of 60–79 years correspond to the oscillation in the global climate system of around 65–70 years cycles [Schlesinger and Ramankutty, 1994; Qian and Lin, 2009]. The centennial cycles of 104–209 years could be associated with variations of solar activity [Braun *et al.*, 2005].

[33] The impacts of decadal- to centennial-scale solar variability on the Asian monsoon variations during the Holocene have been reported basing on many high-resolution climate records both from ocean and continent [Neff *et al.*, 2001;

**Table 6.** The Details of the Compared Series in the Northeastern Tibetan Plateau<sup>a</sup>

Item	Dulan-Zhang	Dulan-Liu	Delingha
Latitude	35°50'~36°30'N	36°3'~36°17'N	36°40'~37°28'N
Longitude	97°40'~98°20'E	98°11'~98°40'E	97°13'~98°25'E
Elevation (m)	3100~3800	3800~4200	3660~3920
Climate signal	May to June precipitation	July to June precipitation	July to June precipitation
Series type	tree ring index	reconstruction	reconstruction
Source	Zhang <i>et al.</i> [2003]	Liu <i>et al.</i> [2006]	Shao <i>et al.</i> [2005]

<sup>a</sup>May to June precipitation is the total precipitation from current May to June. July to June precipitation is the total precipitation from previous July to current June.

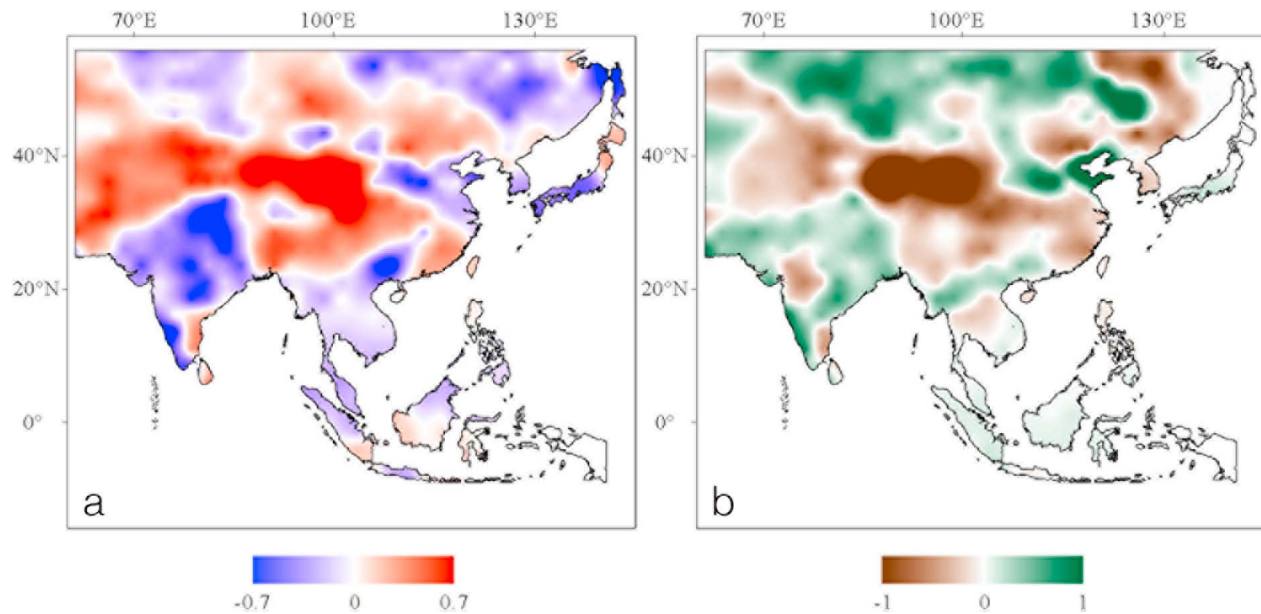


**Figure 7.** (a) Spatial correlation between the precipitation reconstruction in SMQL and the entire grid network of MADA [Cook *et al.*, 2010]. (b) The spatial drought pattern of the great drought during the latter half of the 15th century identified by the MADA [Cook *et al.*, 2010].

[Fleitmann *et al.*, 2003; Wang *et al.*, 2005]. To further reveal the possible relationships between the precipitation variation and solar activity on multidecadal to centennial scales, we compared our precipitation reconstruction with five minimal solar activity periods (Oort Minimum (Om), Wolf Minimum (Wm), Spörer Minimum (Sm), Maunder Minimum (Mm) and Dalton Minimum (Dm)) in Figure 6a. The correspondences between the low-precipitation periods and minimal solar activity periods further reveal the association between the precipitation variation and the solar activity on multidecadal to centennial scale for the last millennium.

## 5. Conclusion

[34] On the basis of the tree ring width indices, we have presented a millennial precipitation reconstruction series in

the south slope of the middle Qilian Mountains, northeastern margin of the Tibetan Plateau. The precipitation reconstruction explains 48.5% of the variance of the instrumental precipitation over the period of 1958 to 2004. The multidecadal dry periods are 1092–1172, 1311–1351, 1441–1517, 1564–1730, and 1814–1878. The wet periods are 1071–1091, 1230–1310, 1352–1440, 1518–1563, 1731–1813, 1879–1941 and 1978–2004. The multidecadal dry and wet events of SMQL have different patterns based on their event scores. All of the stronger dry events, 1092–1172, 1564–1730 and 1441–1517, have higher magnitude or intensity. While the highest scored wet event from 1352 to 1440 is an outstanding wet event among all high-precipitation intervals.

[35] Comparisons with the glacier accumulation and dust content of Dunde ice core confirmed the reliability of the precipitation reconstruction in SMQL. Comparisons with

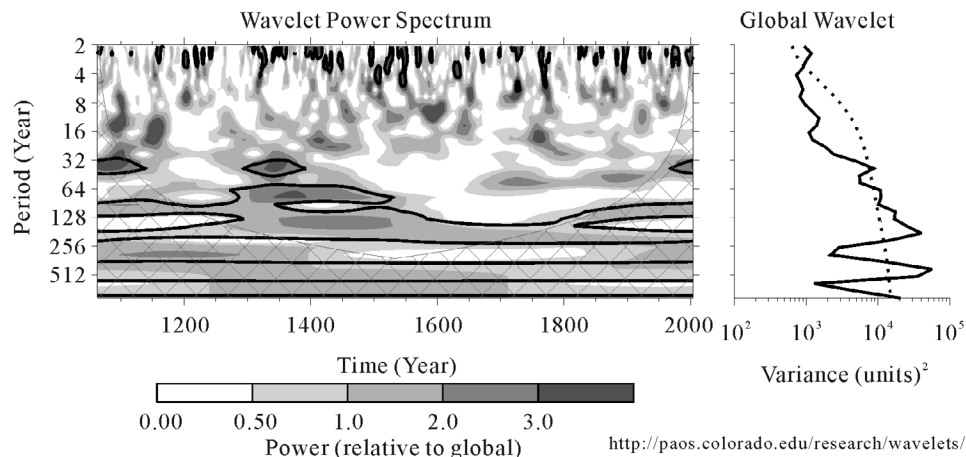


**Figure 8.** Wavelet analyses for the precipitation reconstruction since 1063 AD in SMQL with cone of influence (cross-hatched regions) and significance levels contour of 95%.

other precipitation, runoff and PDSI reconstructions indicate that the precipitation in the northeastern Tibetan Plateau has similar variations over a large spatial and temporal range and the precipitation reconstruction in SMQL can represent the multidecadal-scale moisture conditions in the northeastern Tibetan Plateau for the last millennium, especially during dry periods. The long-lasting severe drought in the latter half of the 15th century further confirms the synchronous occurrence of drought in the northeastern Tibetan Plateau.

[36] Wavelet analyses indicate the dominant periodicities of the precipitation for the last millennium are around 2–3, 39, 60–79, 104–209 years. These mean that the precipitation variations in SMQL could be mainly related to a large-scale atmosphere-ocean system and solar activity on multidecadal to centennial scales in the last millennium. The correspondences between the low-precipitation periods and the minimal solar activity periods further reveal the association with solar activity.

[37] **Acknowledgments.** We thank Xuemei Shao and Qi-bin Zhang for providing the reconstructed precipitation and tree ring index data. We thank the Editor and anonymous reviewers for their great help. We also thank Guang Bao, Bo Sun, Hua Tian, and Tongwen Zhang. This research is supported by grants from the National Basic Research Program of China (2010CB833405), the Chinese NSF (41023006, 40890051, and 40901060), the fund of the Chinese Academy of Sciences (KZZD-EW-04-01, KZZD-EW-TZ-03, and 2007XBBS05), and the State Key Laboratory of Loess and Quaternary Geology. This is a Sino-Swedish Tree Ring Research Center (SISTR) contribution (15).

## References

- Biondi, F., and K. Waikul (2004), DENDROCLIM2002: A C++ program for statistical calibration of climate signals in tree-ring chronologies, *Comput. Geosci.*, **30**, 303–311, doi:10.1016/j.cageo.2003.11.004.
- Biondi, F., T. J. Kozubowski, and A. K. Panorska (2002), Stochastic modeling of regime shifts, *Clim. Res.*, **23**, 23–30, doi:10.3354/cr023023.
- Braun, H., M. Christl, S. Rahmstorf, A. Ganopolski, A. Mangini, C. Kubatzki, K. Roth, and B. Kromer (2005), Possible solar origin of the 1470-year glacial climate cycle demonstrated in a coupled model, *Nature*, **438**, 208–211, doi:10.1038/nature04121.
- Briffa, K. R., T. J. Osborn, F. H. Schweingruber, I. C. Harris, P. D. Jones, S. G. Shiyatov, and E. A. Vaganov (2001), Low-frequency temperature variations from a northern tree ring density network, *J. Geophys. Res.*, **106**, 2929–2941, doi:10.1029/2000JD900617.
- Cook, E. R., and L. A. Kairiukstis (Eds.) (1990), *Methods of Dendrochronology*, Kluwer, Dordrecht, Netherlands.
- Cook, E. R., and K. Peters (1981), The smoothing spline: A new approach to standardizing forest interior tree-ring width series for dendroclimatic studies, *Tree Ring Bull.*, **41**, 45–53.
- Cook, E. R., K. J. Anchukaitis, B. M. Buckley, R. D. D'Arrigo, G. C. Jacoby, and W. E. Wright (2010), Asian monsoon failure and megadrought during the last millennium, *Science*, **328**, 486–489, doi:10.1126/science.1185188.
- Crowley, T. J. (2000), Causes of climate change over the past 1000 years, *Science*, **289**, 270–277, doi:10.1126/science.289.5477.270.
- D'Arrigo, R. D., R. Wilson, and G. Jacoby (2006), On the long-term context for late twentieth century warming, *J. Geophys. Res.*, **111**, D03103, doi:10.1029/2005JD006352.
- Douglass, A. E. (1919), *Climatic Cycles and Tree-Growth*, Carnegie Inst. of Wash., Washington, D. C.
- Durbin, J., and G. S. Watson (1951), Testing for serial correlation in least squares regression, II, *Biometrika*, **38**, 159–178.
- Efron, B. (1979), Bootstrap methods: Another look at the Jackknife, *Ann. Stat.*, **7**, 1–26, doi:10.1214/aos/1176344552.
- Efron, B., and R. Tibshirani (1993), *An Introduction to the Bootstrap*, Chapman and Hall, London.
- Esper, J., E. R. Cook, and F. H. Schweingruber (2002), Low-frequency signals in long tree-ring chronologies for reconstructing past temperature variability, *Science*, **295**, 2250–2253, doi:10.1126/science.1066208.
- Fleitmann, D., S. J. Burns, M. Mudelsee, U. Neff, J. Kramers, A. Mangini, and A. Matter (2003), Holocene forcing of the Indian Monsoon recorded in a stalagmite from southern Oman, *Science*, **300**, 1737–1739, doi:10.1126/science.1083130.
- Fritts, H. C. (1976), *Tree Rings and Climate*, Elsevier, New York.
- Gordon, G. A. (1980), Verification of dendroclimatic reconstructions, in *Climate From Tree Rings*, edited by M. K. Hughes et al., pp. 58–61, Cambridge Univ. Press, Cambridge, U. K.
- Gou, X. H., F. H. Chen, M. X. Yang, and J. B. Li (2005), Climatic response of tree-ring width at different elevations over Qilian Mountains, northwestern China, *J. Arid Environ.*, **61**, 513–524, doi:10.1016/j.jaridenv.2004.09.011.
- Gou, X. H., F. H. Chen, E. Cook, G. Jacoby, M. X. Yang, and J. B. Li (2007), Streamflow variations of the Yellow River over the past 593 years in western China reconstructed from tree rings, *Water Resour. Res.*, **43**, W06434, doi:10.1029/2006WR005705.
- Gray, S. T., S. T. Jackson, and J. L. Betancourt (2004), Tree-ring based reconstructions of interannual to decadal scale precipitation variability for northeastern Utah since 1226 A.D., *J. Am. Water Resour. Assoc.*, **40**(4), 947–960.
- Gray, S. T., J. J. Lukas, and C. A. Woodhouse (2011), Millennial-length records of streamflow from three major Upper Colorado River tributaries, *J. Am. Water Resour. Assoc.*, **47**(4), 702–712.
- Holmes, R. L. (1983), Computer-assisted quality control in tree-ring dating and measurement, *Tree Ring Bull.*, **43**, 69–78.
- Jacoby, G., R. D. D'Arrigo, N. Pederson, B. Buckley, C. Dugarjav, and R. Mijiddorj (1999), Temperature and precipitation in Mongolia based on dendroclimatic investigations, *IAWA J.*, **20**, 339–350.
- Ji, J., J. Shen, W. Balsam, J. Chen, L. W. Liu, and X. Q. Liu (2005), Asian monsoon oscillations in the northeastern Qinghai–Tibet Plateau since the late glacial as interpreted from visible reflectance of Qinghai Lake sediments, *Earth Planet. Sci. Lett.*, **233**(1–2), 61–70, doi:10.1016/j.epsl.2005.02.025.
- Jia, W. X., Y. Q. He, Z. X. Li, H. X. Pang, L. L. Yuan, B. Y. Ning, B. Song, and N. N. Zhang (2008), The regional difference and catastrophe of climatic change in Qilian Mt. region, *J. Geogr. Sci.*, **63**(3), 257–269.
- Jones, P. D., K. R. Briffa, T. P. Barnett, and S. F. B. Tett (1998), High-resolution paleoclimatic records for the last millennium: Interpretation, and comparison with circulation model control-run temperatures, *Holocene*, **8**, 455–471, doi:10.1191/095968398667194956.
- Liu, C. P., T. D. Yao, L. G. Thompson, and M. E. Davis (1999), Variation in microparticle concentrations preserved in the Dunde ice core and its relationship to dust storms and climate since the Little Ice Age, *J. Glaciol. Geocryol.*, **21**(4), 385–390.
- Liu, X. D., and B. D. Chen (2000), Climatic warming in the Tibet Plateau during recent decades, *Int. J. Climatol.*, **20**, 1729–1742, doi:10.1002/1097-0088(20001130)20:14<1729::AID-JOC556>3.0.CO;2-Y.
- Liu, X. H., D. H. Qin, X. M. Shao, T. Chen, and J. W. Ren (2005), Temperature variations recovered in tree-rings in the middle Qilian Mountain over the last millennium, *Sci. China Ser. D, Earth Sci.*, **48**, 521–529.
- Liu, Y., et al. (2006), Precipitation variation in the northeastern Tibetan Plateau recorded by the tree rings since 850 AD and its relevance to the Northern Hemisphere temperature, *Sci. China Ser. D, Earth Sci.*, **49**, 408–420.
- Liu, Y., Z. S. An, H. W. Linderholm, D. L. Chen, H. M. Song, Q. F. Cai, J. Y. Sun, and H. Tian (2009), Annual temperatures during the last 2485 years in the mid-eastern Tibetan Plateau inferred from tree rings, *Sci. China Ser. D, Earth Sci.*, **52**, 348–359.
- Liu, Y., J. Y. Sun, H. M. Song, Q. F. Cai, G. Bao, and X. X. Li (2010), Tree-ring hydrologic reconstruction for the Heihe River watershed, western China since 1430AD, *Water Res.*, **44**, 2781–2792, doi:10.1016/j.watres.2010.02.013.
- Mann, M. E., and P. D. Jones (2003), Global surface temperatures over the past two millennia, *Geophys. Res. Lett.*, **30**(15), 1820, doi:10.1029/2003GL017814.
- Melvin, T. M., and K. R. Briffa (2008), A signal-free approach to dendroclimatic standardization, *Dendrochronologia*, **26**, 71–86, doi:10.1016/j.dendro.2007.12.001.
- Mosteller, F., and J. W. Tukey (1977), *Data Analysis and Regression*, Addison-Wesley, Boston.
- Mudelsee, M. (2003), Estimating Pearson's correlation coefficient with bootstrap confidence interval from serially dependent time series, *Math. Geol.*, **35**, 651–665, doi:10.1023/B:MATG.0000002982.52104.02.
- Neff, U., S. J. Burns, A. Mangini, M. Mudelsee, D. Fleitmann, and A. Matter (2001), Strong coherence between solar variability and the monsoon in Oman between 9 and 6 kyr ago, *Nature*, **411**, 290–293, doi:10.1038/35077048.
- Pederson, N., G. C. Jacoby, R. D. D'Arrigo, E. R. Cook, B. M. Buckley, C. Dugarjav, and R. Mijiddorj (2001), Hydrometeorological reconstructions for Northeastern Mongolia derived from tree rings: AD 1651–1995,

- J. Clim.*, 14(5), 872–881, doi:10.1175/1520-0442(2001)014<0872:HRFNMD>2.0.CO;2.
- Qian, W. H., and X. Lin (2009), An integrated analysis of dry-wet variability in western China for the last 4–5 centuries, *Adv. Atmos. Sci.*, 26(5), 951–961, doi:10.1007/s00376-009-8070-2.
- Qin, C., B. Yang, I. Burchardt, X. L. Hu, and X. C. Kang (2010), Intensified pluvial conditions during the twentieth century in the inland Heihe River Basin in arid northwestern China over the past millennium, *Global Planet. Change*, 72(3), 192–200, doi:10.1016/j.gloplacha.2010.04.005.
- Raspopov, O. M., V. A. Dergachev, and T. Kolström (2004), Periodicity of climate conditions and solar variability derived from dendrochronological and other palaeo-climatic data in high latitudes, *Palaeogeogr. Palaeoclimatol. Palaeoecol.*, 209, 127–139, doi:10.1016/j.palaeo.2004.02.022.
- Schlesinger, M. E., and N. Ramankutty (1994), An oscillation in the global climate system of period 65–70 years, *Nature*, 367, 723–726, doi:10.1038/367723a0.
- Shao, X. M., L. Huang, H. B. Liu, E. Y. Liang, X. Q. Fang, and L. L. Wang (2005), Reconstruction of precipitation variation from tree rings in recent 1000 years in Delingha, Qinghai, *Sci. China Ser. D, Earth Sci.*, 48, 939–949.
- Sheppard, P. R., P. E. Tarasov, L. J. Graumlich, K.-U. Heussner, M. Wagner, H. Osterle, and L. G. Thompson (2004), Annual precipitation since 515 BC reconstructed from living and fossil juniper growth of northeastern Qinghai Province, China, *Clim. Dyn.*, 23, 869–881, doi:10.1007/s00382-004-0473-2.
- Stokes, M. A., and T. L. Smiley (1996), *An Introduction to Tree-Ring Dating*, Univ. of Ariz. Press, Tucson.
- Thompson, L. G., T. D. Yao, M. E. Davis, M.-T. Ellen, T. A. Mashiotta, P. N. Lin, V. N. Mikhalenko, and V. S. Zagorodnov (2006), Holocene climate variability archived in the Puruogangri ice cap on the central Tibetan Plateau, *Ann. Glaciol.*, 43, 61–69, doi:10.3189/172756406781812357.
- Tian, Q. H., X. H. Gou, Y. Zhang, J. F. Peng, J. S. Wang, and T. Chen (2007), Tree-ring based drought reconstruction (A.D. 1855–2001) for the Qilian Mountains, northwestern China, *Tree Ring Res.*, 63, 27–36, doi:10.3959/1536-1098-63.1.27.
- Torrence, C., and G. P. Compo (1998), A practical guide to wavelet analysis, *Bull. Am. Meteorol. Soc.*, 79(1), 61–78, doi:10.1175/1520-0477(1998)079<0061:APGTWA>2.0.CO;2.
- Wang, Y. J., H. Cheng, R. L. Edwards, Y. Q. He, X. G. Kong, Z. S. An, J. Y. Wu, M. J. Kelly, C. A. Dykoski, and X. D. Li (2005), The Holocene Asian Monsoon: Links to solar changes and North Atlantic climate, *Science*, 308, 854–857, doi:10.1126/science.1106296.
- Wigley, T. M. L., K. R. Briffa, and P. D. Jones (1984), On the average value of correlated time series, with applications in dendroclimatology and hydrometeorology, *J. Clim. Appl. Meteorol.*, 23, 201–213, doi:10.1175/1520-0450(1984)023<0201:OTAVOC>2.0.CO;2.
- Yao, T. D., Z. C. Xie, and Q. Z. Yang (1991), Temperature and precipitation fluctuations since 1600 A.D. provided by Dunde Ice Cap, China, paper presented at International Symposium on Glaciers Ocean Atmosphere Interactions, Int. Assoc. of Hydrol. Sci., Moscow.
- Young, G. A. (1994), Bootstrap: More than a stab in the dark, *Stat. Sci.*, 9, 382–395, doi:10.1214/ss/1177010383.
- Yuan, L. (1994), *The Disaster History of the Northwestern China*, Gansu People's Press, Lanzhou, China.
- Zhang, Q. B., G. D. Cheng, T. D. Yao, X. C. Kang, and J. G. Huang (2003), A 2326-year tree-ring record of climate variability on the northeastern Qinghai-Tibetan Plateau, *Geophys. Res. Lett.*, 30(14), 1739, doi:10.1029/2003GL017425.
- Zhang, Q., J. Zhang, G. W. Song, and X. H. Di (2007), Research on atmospheric water-vapor distribution over Qilianshan Mountains, *Acta Meteorol. Sin.*, 65(4), 633–643.

Y. Liu and J. Sun, State Key Laboratory of Loess and Quaternary Geology, Institute of Earth Environment, Chinese Academy of Sciences, Xi'an 710075, China. (liuyu@loess.llqg.ac.cn; sunjy@ieecas.cn)